INTERIOR PENALTY DISCONTINUOUS APPROXIMATIONS OF ELLIPTIC PROBLEMS

RAYTCHO D. LAZAROV, STANIMIRE Z. TOMOV, AND PANAYOT S. VASSILEVSKI

Abstract. This paper studies an interior penalty discontinuous approximation of elliptic problems on non–matching grids. Error analysis, interface domain decomposition type preconditioners, as well as numerical results illustrating both, discretization errors and condition number estimates of the problem and reduced forms of it, are presented.

1. Introduction

In this paper we propose and analyze a simple strategy to construct composite discretizations of self-adjoint second order elliptic equations on generally non–matching grids. The need for discretizations on non–matching grids is motivated partially from devising parallel discretization methods (including adaptive) for PDEs, which is a much easier task if non–matching grids are allowed across the subdomain boundaries. Another situation may arise when different discretizations techniques are utilized in different parts of the subdomains and there is no a priori guarantee that the meshes will be aligned.

Our method can be described as interior penalty approximation based on partially discontinuous elements. The mortar method is a general technique of handling discretizations on non–matching grids. However, our motivation for using the penalty approach, is that it eliminates the need for additional (Lagrange multiplier or mortar) spaces. There is a vast number of publications devoted to the mortar finite element method as a general strategy for deriving discretization methods on non–matching grids. We refer the interested reader to the series of Proceedings of the International Conferences on Domain Decomposition Methods (for more information see, http://www.ddm.org).

In the present paper, we assume a model situation that the domain is split into a fixed number of non–overlapping subdomains and each subdomain is meshed independently. Therefore in general, since the global mesh is not aligned along the

Date: April 19, 1999–beginning; Today is August 25, 2000.

1991 *Mathematics Subject Classification.* 65F10, 65N20, 65N30.

Key words and phrases. non–matching grids, interior penalty discretization, discontinuous elements, error estimates, preconditioning.

The work of the first and the second authors has been partially supported by the US Environmental Protection Agency under Grant R 825207 and by the Natioanl Science Foundation under Grant DMS-9973328. The work of the last author was performed under the auspices of the U. S. Department of Energy by University of California Lawrence Livermore National Laboratory under contract W-7405-Eng-48.

subdomain interfaces, the employed finite element spaces will have functions which are discontinuous along these interfaces. The jump in the values of the functions along these interfaces is penalized in the variational formulation, which is a standard approach in the interior penalty method (cf. [2], [3], [9], [14]). An important feature of our approach, partially motivated by the paper [15], is that we skip the term in the weak formulation that involves the co-normal derivative of the solution to the interface boundaries since the latter may lead to non–symmetric discretization (cf. [14]) of the original symmetric positive definite problem. Thus, for smooth solutions we lose the optimal accuracy due to poor approximation at the interface, but on the other hand produce symmetric and positive definite discrete problem which has optimal condition number.

One can improve the accuracy by increasing the weight in the penalty term on the expense of increased condition number and regularity of the solution, cf., e.g., [8]. Another approach that requires H^2-regularity and has optimal order error estimates, is based on using negative norm in the penalty term (see Remark 3.3). This approach is quite feasible but also increases the condition number and in general requires more involved implementation. Both approaches (increased penalty weight or negative norm penalty terms) will increase the computational complexity of the method. Here we downplay this issue since we believe that an adaptive grid refinement (approach taken in the present paper) is a good alternative. In order to compensate for the low accuracy near the subdomain interfaces we use local grid refinement based on suitable a posteriori error estimators and indicators. Adaptive methods have been extensively used for problems with local singular behavior. Our experience shows that the proposed interior penalty method embedded in a multilevel adaptive grid refinement environment leads to reasonably accurate and fast computations.

For less regular solutions, namely in $H^{1+\epsilon}(\Omega)$, $\epsilon > 0$, the proposed method is also well suited. Such low regularity, for example, will have the solution of an elliptic problem with discontinuous coefficients (interface problem). Finite element Galerkin method with penalty for this class of problems (on matching grids) has been proposed and studied in [3]. Similarly, in [8], the interface problem has been addressed by recasting the problem as a system of first order (by introducing the gradient of the solution as a new vector variable) and applying the least–squares method for the system. Integrals of the squared jumps in the scalar and the normal component of the vector functions on the interface are added as penalty terms in the least–squares functional. In both cases an optimal with respect to the error method leads to a non-optimal condition number of the discrete problem.

Other approaches for handling discretizations on non–matching grids can involve different discretizations in the different subdomains, for example, mixed finite element method in one subdomain and standard Galerkin on the other as proposed in [17] and studied further in [11], or mixed finite element discretizations in both subdomains, cf. e.g., [1], [12].

In this paper we also address the issue of constructing preconditioners for solving the system on the composite non–matching grids. We propose and investigate an

interface domain decomposition type preconditioner (for two subdomains), that is spectrally equivalent to the reduced on the interface algebraic problem.

Finally, the accuracy of the proposed method and the optimal condition number of the the preconditioned problem are demonstrated on a series of numerical experiments on model problems.

The structure of the present paper is as follows. In Section 2 we formulate the problem and its discretization. Section 3 contains the error analysis. The construction and analysis of the interface domain decomposition preconditioners are given in Section 4. The numerical results can found in the final Section 5.

2. Notations and problem formulation

In this paper we use the standard notations for Sobolev spaces of functions defined in a bounded domain $\Omega \subset \mathcal{R}^d$, $d = 2, 3$. For example, $H^s(\Omega)$ for s integer denotes the Hilbert space of functions u defined on Ω and having generalized derivatives up to order s that are square integrable in Ω. For non-integer $s > 0$ the spaces are obtained by the real method of interpolation (cf. [13]). $H_0^1(\Omega)$ is the space of functions in $H^1(\Omega)$ which vanish on $\partial\Omega$. The norm of $u \in H^s(\Omega)$ is denoted by $||u||_{s,\Omega}$. We also use the notation $|u|_{s,\Omega}$ for the semi-norm in $H^s(\Omega)$. For the traces of functions in $H_0^1(\Omega)$ on a manifold Γ of dimension $d-1$ (curves and surfaces) and $\partial\Gamma \subset \partial\Omega$, we use the fractional order Sobolev spaces commonly denoted by $H_{00}^{1/2}(\Gamma)$. The corresponding norm in this space can be characterized, for example as the infimum of the $H^1(\Omega)$-norm of all possible extensions of functions in $H^1(\Omega)$-norm vanishing on $\partial\Omega$.

For a given bounded polygon (polytope) Ω, a source term $f \in L^2(\Omega)$, and coefficient matrix $a(x)$ that is symmetric and uniformly positive definite and bounded in Ω we consider the following boundary value problem for $u(x)$:

$$\left[\begin{array}{rcll} -\nabla \cdot a\nabla u & = & f(x), & x \in \Omega, \\ u(x) & = & g_D(x), & x \in \partial\Omega_D, \\ a\nabla u \cdot \mathbf{n} & = & g_N(x), & x \in \partial\Omega_N, \end{array}\right. \tag{2.1}$$

where $\partial\Omega = \partial\Omega_D \cup \partial\Omega_N$, $\mathbf{n}$ is the unit vector normal to $\partial\Omega$ (pointing outward Ω), $\partial\Omega_D$ has a positive measure, and g_D and g_N are given functions.

To simplify our notation and the overall exposition, we further consider the case of homogeneous Dirichlet data given on the whole boundary $\partial\Omega$, i.e., $\Gamma_N = \emptyset$ ($\Gamma_D = \partial\Omega$) and $g_D = u|_{\Gamma_D} = 0$. However, most of our numerical experiments were done for the general case (2.1).

We shall study a discretization of this problem by the finite element method while using meshes that may not align along certain interfaces. This situation may arise when the domain Ω is split initially into a p nonoverlapping subdomains $\Omega_i, i = 1, \ldots, p$ and each subdomain is meshed (triangulated) independently of the others so that the mesh $\mathcal{T}_i$ is a quasi–uniform triangulation of Ω_i. This means that if $h_T = \mathrm{diam}(T)$ and $|T| = \mathrm{meas}(T)$ then $|T| = h_T^d$, $d = 2, 3$. Further, $\mathcal{T} = \cup_i \mathcal{T}_i$. Denote by Γ_{ij} the interface between two subdomains Ω_i and Ω_j and by Γ the union

of all interfaces Γ_{ij}. We note that there is no assumption that along each interface Γ_{ij} the triangulations $\mathcal{T}_i$ and $\mathcal{T}_j$ produce the same mesh.

We now specify a "master" side of each interface Γ_{ij}, i.e., the mesh from $\mathcal{T}_k$ for k fixed, either equal to i or to j, will generate partition $\mathcal{E}_{ij}$ of Γ_{ij}. Then $e \in \mathcal{E}_{ij}$ defined as $e = \Gamma_{ij} \cap \partial T$, for all $T \in \mathcal{T}_k$. Finally, we define the set of interface "master" elements $\mathcal{E} = \cup_{ij}\mathcal{E}_{ij}$.

Let V_i be the conforming finite element spaces of piece-wise linear functions associated with the triangulation $\mathcal{T}_i$ and let $V : \ V|_{\Omega_i} = V_i, \ i = 1, \ldots, p$, be the finite element space on $\mathcal{T}$. Since the meshes $\mathcal{T}_i$ in Ω_i, $i = 1, \ldots, p$ are generally not aligned along the subdomain interfaces Γ_{ij} the functions $v \in V$ are, in general, discontinuous across Γ_{ij}. However their traces on Γ_{ij} from Ω_i and Ω_j are well–defined.

We now introduce the second order elliptic bilinear forms

$$a_i(v_i, \ \psi_i) = \int_{\Omega_i} a_i \nabla v_i \cdot \nabla \psi_i \ dx, \quad v_i = v|_{\Omega_i}, \ \psi_i = \psi|_{\Omega_i}, \ \text{ for all } v, \ \psi \in H_0^1(\Omega),$$

where, $a_i(x) = a(x)|_{\Omega_i}$ for $i = 1, \ldots, p$. Note, that the form $a_i(\cdot, \cdot)$ is well defined in $V_i \times V_i$.

The weak form of the boundary value problem (2.1) is: Find $u \in H_0^1(\Omega)$ such that

$$a(u, \ \varphi) \equiv \sum_i a_i(u, \ \varphi) = (f, \ \varphi), \quad \text{for all } \varphi \in H_0^1(\Omega). \tag{2.2}$$

For the interior penalty finite element method we shall need some additional constructions. To simplify our notations and exposition we take $d = 2$ (for $d = 3$ in the construction below we have to take $|e|^{1/2}$ instead of $|e|$). First, we introduce the following bilinear form on $V \times V$:

$$b_h(v_h, \varphi) = \sum_{e \in \mathcal{E}} \frac{\sigma(e)}{|e|} \int_e [v_h]_e [\varphi]_e \ d\varrho. \tag{2.3}$$

Here, $[\varphi]_e$ is the jump of φ across $e \in \mathcal{E}_{ij} \subset \mathcal{E}$, i.e. $[\varphi]_e = \varphi_i|_e - \varphi_j|_e$ where $\mathcal{E}_{ij}$ is a partition of Γ_{ij} obtained from the master triangulation $\mathcal{T}_k$ ($k = i$ or $k = j$) and $|e|$ is the measure of e. Since the triangulations $\mathcal{T}_i$ are assumed quasi–uniform, we have that $|e| \simeq h_k$.

The weight $\sigma(e)$ can be defined in various ways with the simplest $\sigma(e) = 1$. Better numerical results in the case of coefficients with large jumps across the interface Γ or anisotropy gives the following weight, which uses harmonic averages of the coefficient matrix $a(x)$:

$$\sigma(e) = \frac{2}{\kappa_i + \kappa_j}, \ \kappa_l = \frac{1}{|e|} \int_e a_l^{-1}(x) \mathbf{n}_e(x) \cdot \mathbf{n}_e(x) \ d\varrho, \ l = i, j,$$

where $\mathbf{n}_e(x)$ denotes the unit normal vector to e at the point $x \in e$.

We study the following discretization method (called further interior penalty discretization):

Find $u_h \in V$ such that

$$a_h(u_h,\ \varphi) \equiv a(u_h,\ \varphi) + b_h(u_h,\ \varphi) = (f,\ \varphi), \quad \text{for all } \varphi \in V. \tag{2.4}$$

Since the finite element space contains functions that are discontinuous across Γ the penalty form $b_h(\cdot,\cdot)$ imposes a weak compatibility of the solution across Γ, i.e., it controls the size of the jump $[u_h]_e$.

The bilinear from $a_h(\cdot,\cdot)$ defined in (2.4) is symmetric and positive definite. It is related but much simpler than the corresponding discontinuous Galerkin method used in [2], [14]. The simplification comes from the fact that we have disregarded the term involving the co-normal derivative $a\nabla u \cdot \mathbf{n}$ along the interface Γ with unit normal vector $\mathbf{n}$. This simplification comes with a cost: the proposed approximation will not have optimal order of convergence, in contrast to the nonsymmetric interior penalty Galerkin method, studied in [14]. However, our formulation leads to a symmetric and positive definite problem and combined with local grid refinement generated by an a posteriori analysis produces efficient and accurate computational method as demonstrated by our numerical experiments.

3. Error estimates

In this section we derive the basic error estimates for the proposed interior penalty method (2.4). We assume that the following two conditions:

(A.1) The solution $u(x)$ of (2.2) is $H^{\frac{3}{2}+\alpha}(\Omega)$-regular, with $\alpha > 0$;

(A.2) The solution $u(x)$ of (2.2) satisfies the estimate $\|u\|_{\frac{3}{2}+\alpha,\Omega} \leq C\|f\|_{0,\Omega}$;

(A.3) The maximum step-size of $\mathcal{T}_i$ is h_i and $h_i \simeq h$, for $i = 1, \ldots, p$.

The condition (A.3) means that the mesh $\mathcal{T}$ is a global quasi–uniform partition of Ω.

For $u_h \in V$ we define the "energy" norm $||u_h||^2_{1,h} = a_h(u_h, u_h)$. Obviously this norm is well defined for $u \in H^1_0(\Omega)$ and $||u||^2_{1,h} = a(u, u)$.

The following theorem is the main result in this section:

Theorem 3.1. *Assume that the conditions (A.1), (A.3) hold. Then*

$$||u - u_h||_{1,h} \leq C_1 h^{1/2} ||u||_{\frac{3}{2}+\alpha,\Omega}. \tag{3.1}$$

If in addition (A.2) holds, then

$$||u - u_h||_{0,\Omega} \leq C_0 h ||u||_{\frac{3}{2}+\alpha,\Omega}. \tag{3.2}$$

The constants C_0 and C_1 are independent of h and $\alpha > 0$.

Remark 3.1. *The condition (A.1) requires a little bit more regularity than the standard Galerkin method, where $H^{1+\epsilon}(\Omega)$-regularity gives $\mathcal{O}(h^\epsilon)$ convergence rate in energy norm. We can make our analysis work for this case as well. However, we prefer to keep the exposition on simple level and to avoid all technicalities when working with the trace of $a\nabla u \cdot \mathbf{n}$ in Sobolev spaces with negative index.*

Proof. We first note that the exact solution u satisfies the identity,

$$a(u,\ \varphi) = (f,\ \varphi) + \int_\Gamma a\nabla u \cdot \mathbf{n}[\varphi]\ d\varrho, \quad \text{for all } \varphi \in V.$$

We here used the that the exact solution has continuous (in a weak sense) normal flux, i.e., in particular, $[a\nabla u \cdot \mathbf{n}]|_\Gamma = 0$.

Similarly, the discrete solution u_h solves the problem,

$$a_h(u_h,\ \varphi) = \sum_i a_i(u_h,\ \varphi) + b_h(u_h,\ \varphi) = (f,\ \varphi) \quad \text{for all } \varphi \in V.$$

Let ψ_h be the nodal interpolant of the exact solution in V. Note, that ψ_h is discontinuous on Γ, but its jump $[\psi_h]$ is small, since u is a continuous function in Ω.

¿From the above identities for u and u_h it is clear then that $\delta_h = u_h - \psi_h$ solves the discrete problem,

$$\begin{aligned} a(\delta_h,\ \varphi) + &\sum_{e\in\mathcal{E}} \frac{\sigma(e)}{|e|}\int_e [\delta_h]_e[\varphi]_e\ d\varrho \\ &= a(u-\psi_h,\ \varphi) - \int_\Gamma a\nabla u\cdot\mathbf{n}[\varphi] d\varrho - \sum_{e\in\mathcal{E}} \frac{\sigma(e)}{|e|}\int_e [\psi_h]_e[\varphi]_e\ d\varrho, \end{aligned}$$

for all $\varphi \in V$.

Taking into account that $-[\psi_h]_e = [u-\psi_h]_e$ and using the definition of $a_h(\cdot,\cdot)$ we rewrite this equation in the form:

$$a_h(\delta_h,\ \varphi) = a_h(u-\psi_h,\ \varphi) - \int_\Gamma a\nabla u\cdot\mathbf{n}\ [\varphi]\ d\varrho.$$

Now choosing $\varphi = \delta_h$ and applying Schwarz inequality to both terms on the right, we get

$$\begin{aligned} a_h(\delta_h,\ \delta_h) \ &\le [a_h(u-\psi_h,\ u-\psi_h)\ a_h(\delta_h,\ \delta_h)]^{1/2} \\ &+ \left(\sum_{e\in\mathcal{E}} \frac{|e|}{\sigma(e)}\int_e (a\nabla u\cdot\mathbf{n})^2\ d\varrho\right)^{1/2} \left(\sum_{e\in\mathcal{E}} \frac{\sigma(e)}{|e|}\int_e [\delta_h]_e^2\ d\varrho\right)^{1/2}, \end{aligned}$$

which after applying the inequality $a_1b_1 + a_2b_2 \le \sqrt{a_1^2+a_2^2}\sqrt{b_1^2+b_2^2}$ yields,

$$a_h(\delta_h,\ \delta_h) \le \left[a_h(u-\psi_h,\ u-\psi_h) + \sum_{e\in\mathcal{E}} \frac{|e|}{\sigma(e)}\int_e (a\nabla u\cdot\mathbf{n})^2\ d\varrho\right]^{\frac{1}{2}} [2a_h(\delta_h,\ \delta_h)]^{\frac{1}{2}}.$$

Using this inequality and taking into account that $e_h \equiv u - u_h = u - \psi_h - \delta_h$ we get the following basic bound for the error e_h:

$$
\begin{aligned}
||e_h||^2_{1,h} &\equiv a_h(e_h,\ e_h) \le 2a_h(u-\psi_h,\ u-\psi_h) + 2a_h(\delta_h,\ \delta_h) \\
&\le 4a_h(u-\psi_h,\ u-\psi_h) + 2\sum_{e\in\mathcal{E}} \frac{|e|}{\sigma(e)} \int_e (a\nabla u\cdot\mathbf{n})^2\, d\varrho \\
&\equiv 4a(u-\psi_h,\ u-\psi_h) + 4\sum_{e\in\mathcal{E}} \frac{\sigma(e)}{|e|} \int_e [u-\psi_h]_e^2\, d\varrho \\
&\qquad +2\sum_{e\in\mathcal{E}} \frac{|e|}{\sigma(e)} \int_e (a\nabla u\cdot\mathbf{n})^2\, d\varrho.
\end{aligned} \tag{3.3}
$$

Since the solution $u(x)$ is $H^{\frac{3}{2}+\alpha}(\Omega)$-regular, $\alpha > 0$, the last term is easily bounded by the trace theorem

$$
\sum_{e\in\mathcal{E}} \frac{|e|}{\sigma(e)} \int_e (a\nabla u\cdot\mathbf{n})^2\, d\varrho \le Ch\|\nabla u\cdot\mathbf{n}\|^2_{0,\Gamma} \le Ch\|u\|^2_{\frac{3}{2}+\alpha,\Omega}. \tag{3.4}
$$

Note, that this term gives the largest contribution to the error. We show below that all other terms in the right hand side of (3.3) are asymptotically smaller.

A bound for the term $a_h(u-\psi_h,\ u-\psi_h)$ is a corollary of the standard error estimate for the interpolant ψ_h of u on V:

$$
a(u-\psi_h,\ u-\psi_h) = \sum_i a_i(u-\psi_h,\ u-\psi_h) \le Ch^{3+2\alpha}|u|^2_{\frac{3}{2}+\alpha,\Omega}. \tag{3.5}
$$

We now consider the second term on the right-hand side of (3.3). First, we note that

$$
\begin{aligned}
\sum_{e\in\mathcal{E}} \frac{\sigma(e)}{|e|} \int_e [u-\psi_h]_e^2\, d\varrho &\le Ch^{-1} \sum_{\mathcal{E}_{ij}\subset\mathcal{E}} \int_{\Gamma_{ij}} [u-\psi_h]^2\, d\varrho \\
&\le Ch^{-1} \sum_{\mathcal{E}_{ij}\subset\mathcal{E}} \int_{\Gamma_{ij}} \Big((u-\psi_h)|_{\Gamma_{ij}\cap\partial\Omega_i} - (u-\psi_h)|_{\Gamma_{ij}\cap\partial\Omega_j} \Big)^2 d\varrho \\
&\le Ch^{-1} \sum_{l=1}^{p} \int_{\partial\Omega_l} (u-\psi_h)^2 d\varrho.
\end{aligned} \tag{3.6}
$$

Fix l, $1 \le l \le p$. Let T be an element of $\mathcal{T}_l$, such that $e_l = \partial T \cap \partial\Omega_l$ is an edge of T. Since the triangulation $\mathcal{T}_l$ is quasi–uniform we have $|e_l| \simeq Ch_T$ and $|T| \simeq Ch_T^2$. We next recall the following (trace type) inequality

$$
\frac{1}{|e_l|} \int_{e_l} \varphi^2\, d\varrho \le C \left[\frac{1}{|T|}\|\varphi\|^2_{0,\,T} + \frac{h^{1+2\alpha}}{|T|}|\varphi|^2_{\frac{1}{2}+\alpha,T} \right], \text{ for } \varphi \in H^{\frac{1}{2}+\alpha}(T), \tag{3.7}
$$

which is verified first for a domain of unit size and then by transforming T to a domain of unit size to get the appropriate scaling.

Summing (3.7) over all edges of $T \in \mathcal{T}_l$ along $\partial\Omega_l$, and using the approximation properties of the space V_l (ψ_h is the nodal interpolant of u in V) we get

$$
\begin{aligned}
h^{-1}\int_{\partial\Omega_l}(u-\psi_h)^2 d\varrho &\leq C\left(h^{-2}\|u-\psi_h\|^2_{0,\,\Omega_l} + \|u-\psi_h\|^2_{1,\,\Omega_l}\right) \\
&\leq Ch^{1+2\alpha}||u||^2_{\frac{3}{2}+\alpha,\Omega_l}
\end{aligned} \tag{3.8}
$$

and the final result follows by summation over l.

Remark 3.2. *Note that the mesh-sizes in the above formula are local near Γ, so applying local refinement (see Subsection 5.3) for small additional cost for smooth solutions one gets "first order" accurate scheme. Part of the additional cost is the increasing condition number, which may be a problem if no preconditioning is used. If the penalty term is increased, for example, by additionally multiplying by $\frac{1}{|e|}$ one gets first order scheme provided that the solution is smooth along Γ. In that case a new preconditioner has to be found.*

We now continue with bounding the error in L^2–norm, which is obtained by a standard duality argument. Consider the dual problem:

Find $z \in H^1_0(\Omega)$ such that $a(z,\varphi) = (e_h,\varphi)$ for every $\varphi \in H^1_0(\Omega)$. Let $z_h \in V$ be the discrete solution of the dual problem obtained by the described above penalty method, i.e. $a_h(z_h,\varphi) = (e_h,\varphi)$ for all $\varphi \in V$.

Use now the fact that z_h and u_h are the solution of the discrete problems approximating z and u respectively, one gets,

$$
\begin{aligned}
\|e_h\|^2_0 &= a(z,\ e_h) + \int_\Gamma a\nabla z\cdot\mathbf{n}\,[e_h]d\varrho \\
&= a(z-z_h,\ e_h) + a(z_h,\ e_h) + \int_\Gamma a\nabla z\cdot\mathbf{n}\,[e_h]d\varrho \\
&\leq \|z-z_h\|_{1,h}\|e_h\|_{1,h} - b_h(z_h,\ u-u_h) + \int_\Gamma a\nabla u\cdot\mathbf{n}\,[z_h]d\varrho + \int_\Gamma a\nabla z\cdot\mathbf{n}\,[e_h]d\varrho.
\end{aligned}
$$

Thus, from the Cauchy–Schwarz inequality and the energy error estimate (3.1), we have

$$
\begin{aligned}
-b_h(z_h,\ u-u_h) &= b_h(z-z_h,\ u-u_h) \\
&\leq [b_h(z-z_h,\ z-z_h)b_h(u-u_h,\ u-u_h)]^{\frac{1}{2}} \\
&\leq \|z-z_h\|_{1,h}\|u-u_h\|_{1,h} \\
&\leq Ch^{\frac{1}{2}}\|z\|_{\frac{3}{2}+\alpha,\Omega}\|e_h\|_{1,h}.
\end{aligned}
$$

One also has, using the Cauchy–Schwarz, the trace inequality, the energy error estimate (3.1) for $z-z_h$, and assumption (A.2)

$$
\begin{aligned}
\textstyle\int_\Gamma a\nabla u\cdot\mathbf{n}\,[z_h]d\varrho &\leq Ch^{\frac{1}{2}}\left[\int_\Gamma (a\nabla u\cdot\mathbf{n})^2\,d\varrho\right]^{\frac{1}{2}}[b_h(z-z_h,\ z-z_h)]^{\frac{1}{2}} \\
&\leq Ch\|u\|_{\frac{3}{2}+\alpha,\Omega}\|z\|_{\frac{3}{2}+\alpha,\Omega} \leq Ch\|u\|_{\frac{3}{2}+\alpha,\Omega}\|e_h\|_0.
\end{aligned}
$$

Finally, apply again the trace inequality and assumption (A.2) to get

$$\int_\Gamma (a\nabla z \cdot \mathbf{n})^2 \, d\varrho \le C\|z\|^2_{\frac{3}{2}+\alpha,\Omega} \le C||e_h||^2_0.$$

Using these estimates we get

$$||e_h||^2_0 \le C\left(h^{\frac{1}{2}}||z||_{\frac{3}{2}+\alpha,\Omega}||e_h||_{1,h} + h||z||_{\frac{3}{2}+\alpha,\Omega}\,||u||_{\frac{3}{2}+\alpha,\Omega}\right) \le Ch||u||_{\frac{3}{2}+\alpha,\Omega}\,||e_h||_0,$$

which yields (3.2). □

Remark 3.3. *One can achieve optimal order error estimates if the penalty term is taken in negative norm which will allow a different penalty weight to be used. More precisely, one may use the following negative norm interior penalty boundary form:*

$$\frac{1}{h^{1+2\alpha}}\ \left\langle \Lambda_h^{-\alpha}[v],\ [w]\right\rangle_\Gamma .$$

For simplicity assume two subdomains, $p = 2$ and let $k = 1$ be the master side of the boundary $\Gamma = \Gamma_{12}$. Then $\Lambda_h :\ V_1 \mapsto V_1$ defines an $H^1_0(\Gamma)$-equivalent norm on $V_1|_\Gamma$. For $\alpha \in [0, \frac{1}{2}]$ one gets a scale of interior penalty forms. By a straightforward modification of the above error analysis one can get a $\mathcal{O}(h^{\frac{1}{2}+\alpha})$ error estimates in energy norm for $u \in H^{\frac{3}{2}+\alpha}(\Omega)$. Unfortunately, the condition number of the resulting matrices increases to $\mathcal{O}(h^{-2-2\alpha})$, instead of $\mathcal{O}(h^{-2})$, the condition number of the unpenalized problem. Also, use of negative norm penalty forms raises the question of computing the actions of the corresponding boundary operator, which in general gives rise to dense matrices. If one assumes a multilevel structure of the mesh in Ω_1, then one potential candidate for $\Lambda_h^{-\alpha}$ which is inexpensively computable can come from the (boundary) Sobolev norms of negative fractional order studied in [7]. *It is clear that use of negative norm operators leads to more involved implementation and in the present paper we have taken the somewhat simpler approach of utilizing local refinement near the interface boundary in order to control the accuracy.*

4. Iterative solution of the resulting linear system

In this section we study some preconditioning technique for solving the system of algebraic equations produced by the interior penalty method. Here we shall study the case $p = 2$, so that $\Gamma_{12} = \Gamma$, and assume that Γ intersects $\partial\Omega$.

We next introduce the reduced problem on the interface Γ, which corresponds to eliminating the interior for Ω_1 and Ω_2 nodes thus leading to an interface Schur complement system for the unknowns on Γ.

First, we introduce the Schur complement operators $S_i :\ V_i|_\Gamma \mapsto\ V_i|_\Gamma$, $i = 1, 2$:

$$(S_i\psi_i,\ \psi_i) \equiv \inf_{v_i \in V_i:\ v_i|_\Gamma = \psi_i} a_i(v_i,\ v_i),$$

where the pairing $(\cdot, \cdot)$ here represents integration on Γ.

Next, we introduce the reduced system on the interface Γ: Find $\varphi_i \in V_i|_\Gamma$, such that,

$$(S_1\varphi_1,\ \psi_1) + (S_2\varphi_2,\ \psi_2) + b_h(\varphi,\ \psi) = (g,\ \psi), \quad \text{for all } \psi \in V. \tag{4.1}$$

One can further reduce the problem, by looking at the Schur complement

$$(\sigma_1\varphi_1,\ \varphi_1) = \inf_{\varphi_2}\ \left[(S_2\varphi_2,\ \varphi_2) + b_h(\varphi,\ \varphi)\right]. \tag{4.2}$$

so that the final reduced on Γ problem reads,

$$(S_1\varphi_1,\ \psi_1) + (\sigma_1\varphi_1,\ \psi_1) = (g_1,\ \psi_1), \quad \text{for all } \psi_1. \tag{4.3}$$

Obviously, $S_1 + \sigma_1 :\ V_1|_\Gamma \mapsto\ V_1|_\Gamma$ is a symmetric an positive definite operator

The following main result holds:

Theorem 4.1. *The reduced boundary operator $S_1 + \sigma_1$ is spectrally equivalent to its principal part S_1, that is*

$$(S_1\psi_1,\ \psi_1) \le ((S_1 + \sigma_1)\psi_1,\ \psi_1) \le C(S_1\psi_1,\ \psi_1), \quad \textit{for all } \psi_1$$

with a constant independent of h and on $\frac{h_1}{h_2}$.

Proof. We only have to prove that σ_1 is bounded in terms of S_1. Note that S_1 defines a norm equivalent to $H^{\frac{1}{2}}_{00}(\Gamma)$ restricted to the traces of the finite element space V_1. ¿From the definition of σ_1, one has,

$$(\sigma_1\psi_1,\ \psi_1) \le (S_2\psi_2,\ \psi_2) + b_h(\psi,\ \psi), \quad \text{for all } \psi_2.$$

Choose now, $\psi_2 = Q_2^h\psi_1$ where Q_2^h is the L^2–projection onto V_2. In order to define $Q_2^h\psi_1$ we assume that ψ_1 has been harmonically extended in Ω_2, which means that the $H^1(\Omega_2)$-norm of the extension is bounded by the $H^{\frac{1}{2}}_{00}(\Gamma)$-norm of ψ_1. Then the boundary term is estimated as follows, using inequality (3.7), the L^2-approximation and H^1–boundedness properties of Q_2^h, and the fact that $|e| \simeq h_2$,

$$\begin{aligned} b_h(\psi,\ \psi) &= \sum_{e\in\mathcal{E}} \tfrac{\sigma(e)}{|e|} \int_e \left[(I - Q_2^h)\psi_1\right]^2\ d\varrho \\ &\le C\left[|e|^{-2}\|(I - Q_2^h)\psi_1\|^2_{0,\,\Omega_2} + \|(I - Q_2^h)\psi_1\|^2_{1,\Omega_2}\right] \\ &\le C\|\psi_1\|^2_{1,\,\Omega_2} \le C\|\psi_1\|^2_{\frac{1}{2},\,\Gamma} \le C(S_1\psi_1,\ \psi_1). \end{aligned}$$

The rest is also straightforward. One has,

$$\begin{aligned} (S_2\psi_2,\ \psi_2) &\le a_2(Q_2^h\psi_1,\ Q_2^h\psi_1) \le C\|Q_2^h\psi_1\|^2_{1,\,\Omega_2} \\ &\le C\|\psi_1\|^2_{1,\,\Omega_2} \le C\|\psi_1\|^2_{\frac{1}{2},\,\Gamma} \le C(S_1\psi_1,\ \psi_1). \end{aligned}$$

□

Remark 4.1. *In order to compute the actions of σ_1 one has to solve the variational problem* (4.2)*. This is equivalent to solve the following sub-domain problem, for a*

given φ_1 *on* Γ,

$$a_2(\varphi_2,\ \psi_2) + \sum_{e\in\mathcal{E}} \frac{\sigma(e)}{|e|} \int_e \varphi_2\psi_2\ d\varrho = \sum_{e\in\mathcal{E}} \frac{\sigma(e)}{|e|} \int_e \varphi_1\psi_2\ d\varrho, \quad \textit{for all } \psi_2 \in V_2.$$

Obviously, the condition number of the resulting matrix depends on the size of $|e|$, $e \in \mathcal{E}$. *It is clear that if* $\mathcal{E}$ *was based on* $\mathcal{T}_2$, *then the condition number of above system would have been independent of* h_1. *The actions of* σ_1 *can be computed using the preconditioned CG method exploiting (a variant of) the preconditioner for interior penalty bilinear form studied in* [15].

5. Numerical results

The performance of the proposed penalty method is described in the following six subsections. In Subsection 5.1 we give results for non–matching and matching grids. In Subsection 5.2, we have incorporated a weight $\delta > 0$ in the penalty term, and studied its effect on the accuracy and on the condition number of the resulting matrices. Subsection 5.3 deals with locally refined meshes obtained as a result of a posteriori error analysis in order to improve on the accuracy of the method. In Subsection 5.4 the same numerical results as in Subsection 5.1 are given, now for varying coefficients a_i. Finally, in Subsection 5.5, condition number estimates for the original problem (2.4), as well as for the reduced problems (4.1) and (4.3). The same is done for the preconditioned reduced problem (4.3), by the described in Section 4 interface domain decomposition type preconditioner S_1.

Our finite element implementation handles arbitrary triangulations of the domain and linear finite elements. The embedded into the code refinement techniques yield a sequence of nested triangulations which are used to define multilevel preconditioners for the subdomain problems.

In all tables we present the computational results for various test problems with smooth solutions. The domain is split into two subdomains that are triangulated independently so that the meshes do not match along the interface Γ. In Tables 1, 2, 5, and 6 we present the number of nodes for each level of grid refinement, the error in maximum (L^∞), L^2 and H^1-norm, and the condition number of the algebraic system for the penalty approximation. The results are given for each subdomain separately, in each box the first line is for the bigger domain and the second line is for the smaller one.

5.1. **Uniform refinement results on non-matching grids.** In the first test we use the mesh shown in Figure 1. The grids are non-matching along the interface between the sub-domains Ω_1 (upper left part of Figure 1) and Ω_2 (lower right corner). The exact solution is $u(x, y) = x^2 - y^2$, and the coefficients are $a_1 = a_2 = I$. Dirichlet boundary conditions are imposed on the lines $x = 0$, $y = 0$, and Neumann boundary conditions on the lines $x = 1$, $y = 1$. The symmetric and positive definite discrete problem is solved using the CG method.

In Figure 1, in addition to the mesh, we have given the approximate solution and the error on refinement level 2. Table 1 summarizes the numerical results. The last

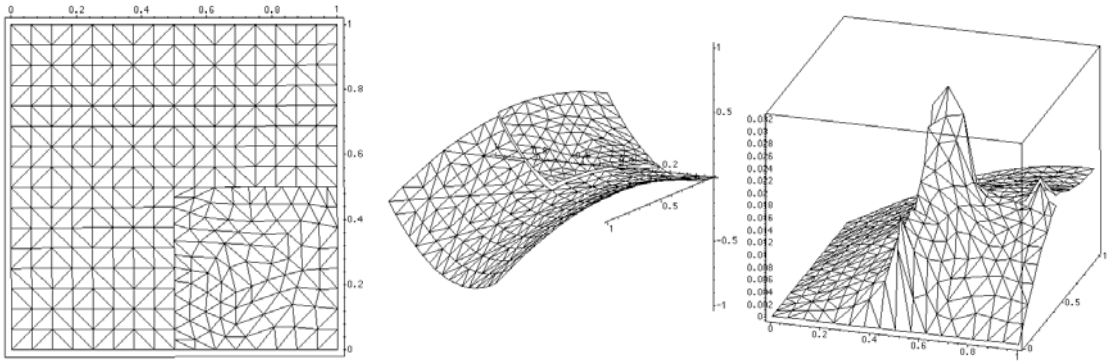

FIGURE 1. Mesh on level 2 (left), the approximate solution on level 2 (middle) and the error on level 2 (right)

column gives the condition number of the discrete problem. The error on the finest

Uniformly refined grid					
level	# nodes	L^∞-error	L^2-error	H^1-error	condition #
1	65	0.027682	0.009983	0.095231	149
	31	0.038660	0.009136	0.069610	
2	225	0.015073	0.005105	0.049991	519
	102	0.022372	0.004702	0.038111	
3	833	0.008204	0.002527	0.025563	2278
	367	0.011481	0.002291	0.019864	
4	3201	0.004255	0.001263	0.013130	9781
	1389	0.005830	0.001131	0.010353	
5	12545	0.002176	0.000632	0.006796	40083
	5401	0.002940	0.000566	0.005512	
order	2	$\approx$ 1	$\approx$ 1	$\approx$ 1	2

TABLE 1. Numerical results for uniform refinement; non-matching grids.

(5th) level is 0.22%, 0.20% and 0.47% correspondingly in the discrete maximum, L^2 and H^1-norms.

To make an assessment of the performance of the penalty method we solved the same problem on matching grids uniformly refined to level 5. The results of these computations are presented in Table 2. Comparing Table 1 and Table 2 one can see that the condition numbers and the accuracy are very close. The error on the finest (5th) level is 0.35%, 0.34% and 0.57% correspondingly in the discrete maximum-norm, L^2-norm and H^1-norm.

5.2. **Variable penalty weight.** Here we test the effect on the accuracy and condition number of the resulting discrete problems, of varying the penalty weight δ

Uniformly refined grid					
level	# nodes	L^∞-error	L^2-error	H^1-error	condition #
1	65	0.039405	0.016707	0.106070	143
	25	0.054990	0.016297	0.084409	
2	225	0.022533	0.008476	0.056189	498
	81	0.027814	0.008517	0.046363	
3	833	0.012380	0.004281	0.029705	1829
	289	0.014366	0.004374	0.025188	
4	3201	0.006617	0.002154	0.015650	6982
	1089	0.007399	0.002221	0.013546	
5	12545	0.003456	0.001081	0.008212	27247
	4225	0.003770	0.001120	0.007223	
order	2	$\approx$ 1	$\approx$ 1	$\approx$ 1	2

TABLE 2. Numerical results for uniform refinement; matching grids.

incorporated in front of the interior penalty boundary form,

$$a(u_h,\ \varphi) + \delta \sum_{e\in\mathcal{E}} \frac{\sigma(e)}{|e|} \int_e [u_h]_e[\varphi]_e \, d\varrho = (f,\ \varphi) + \int_{\Gamma_N} g_N \varphi d\varrho, \quad \text{for all } \varphi \in V.$$

On Γ_D we take u_h equal to the piece-wise linear interpolant of the boundary data g_D.

The domain is as in the previous subsections and Dirichlet boundary conditions are applied on the whole boundary $\partial\Omega$. In Table 3 we give the results for varying δ on non–matching grids, and in Table 4 are the results for the case of matching grids. The meshes are kept fixed. The non–matching grid has 833 nodes in subdomain Ω_1 and 231 nodes in Ω_2, corresponding to $h = 0.04$ ($h^{-\frac{1}{2}} = 5$). The matching grid has 833 nodes in Ω_1 and 289 nodes in Ω_2. The computations for both, matching and non–matching grids, show that increasing δ puts more weight on the penalty term and leads to decreasing the errors in all norms. However, for δ larger than $h^{-1/2}$ there is no significant improvement in the accuracy. This is in agreement with the presented above theory. Moreover, for non–matching grids very large δ causes deterioration of the error in maximum and H^1-norm and, as expected, increases the condition number.

5.3. **Local refinement results.** We here consider the problem from Subsection 5.1. There is a wide range of well–established a posteriori local error estimators that are used to generate locally refined meshes that guarantee accurate discretizations, e.g., *Residual based refinement* [4], [6], [16], *Zienkiewicz-Zhu error estimator* [18], *Hierarchical refinement* [5], and *Second derivative refinement* [10].

In our context we had to adapt the estimators near Γ due to the interior penalty form. The grids obtained as a result of applying the above four error estimators differ slightly, but in all cases of smooth solutions the estimators lead to meshes

δ	L^∞-error	L^2-error	H^1-error	condition #
0.1	0.255030	0.141213	0.497448	420
	0.605293	0.227123	0.642739	
1	0.049788	0.019099	0.135558	420
	0.088299	0.029629	0.132201	
$h^{-1/2}$=5	0.013678	0.004131	0.092995	1190
	0.020614	0.006253	0.074047	
10	0.007464	0.002485	0.089832	2273
	0.011123	0.003379	0.069903	
1000	0.013250	0.002558	0.093995	88288
	0.011979	0.002308	0.075255	

TABLE 3. Numerical results for varying δ; non-matching fixed grids.

δ	L^∞-error	L^2-error	H^1-error	condition #
0.1	0.080767	0.024755	0.159351	440
	0.184311	0.039591	0.203872	
1	0.012907	0.003594	0.036052	440
	0.022984	0.005555	0.035535	
$h^{-1/2} = 5$	0.003310	0.000759	0.023133	615
	0.004671	0.001158	0.014892	
10	0.001778	0.000417	0.022384	1162
	0.002340	0.000590	0.013363	
1000	0.000019	0.000173	0.022098	42261
	0.000024	0.000100	0.012758	

TABLE 4. Numerical results for varying δ; matching fixed grids.

that are refined in the areas around the interior boundary. Here we present the results from the *Residual based refinement* estimator only. The method is based on equilibrating certain residuals over the elements. The residual over one element is decomposed into two parts. The first part contains the contribution of the interior of the finite element and the second part consists of the contribution from jumps of the normal flux across the finite element boundary.

More specifically, in our computations for every element $T \in \mathcal{T}_i$ we compute and equilibrate the following quantities:

$$\rho_T \equiv h_T ||f + \nabla \cdot a \nabla u_h||_T + h_T^{1/2} \sum_{e \in \partial T} R_e \ ,$$

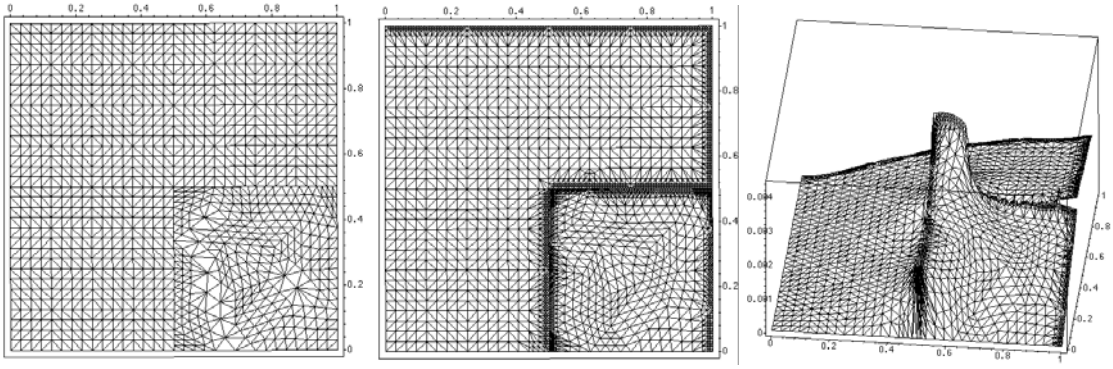

FIGURE 2. Mesh on level 2 (left), mesh on level 4 (middle) and the error on level 4 (right).

where the residuals R_e are defined as

$$R_e = \begin{cases} 0 & \text{if } e \in \partial\Omega_D \ , \\ ||g_N - a\nabla u_h \cdot \mathbf{n}||_e & \text{if } e \in \partial\Omega_N \ , \\ \frac{1}{2}||[a\nabla u_h] \cdot \mathbf{n}||_e & \text{if } e \in \Omega \setminus \{\partial\Omega \cup \Gamma\}, \\ \frac{1}{2}||[a\nabla u_h] \cdot \mathbf{n}||_e + ||a\nabla u_h \cdot \mathbf{n}||_e & \text{if } e \in \Gamma. \end{cases} \tag{5.1}$$

Asymptotically this error indicator, as the a priori estimate, is of order $1/2$ because of the term $||a\nabla u_h \cdot \mathbf{n}||_e$. Equilibration of ρ_T ensures that the term $h_1 \int_\Gamma (a\nabla u \cdot \mathbf{n})^2 \, d\varrho$ (see, the error estimates in Theorem 3.1) will be of size Ch^2, where h is the quasi–uniform size of the mesh away from Γ, i.e. due to the local refinement we should get close to a first order scheme.

level	# nodes	L^∞-error	L^2-error	H^1-error	condition #
1	225	0.022438	0.007905	0.052656	521
	102	0.032274	0.007905	0.052656	
2	833	0.012507	0.003926	0.027194	2328
	307	0.016949	0.003248	0.024047	
3	1139	0.006597	0.002000	0.022904	5036
	589	0.008623	0.001591	0.015972	
4	1759	0.003334	0.001017	0.021487	9814
	1109	0.004390	0.000802	0.013027	

TABLE 5. Numerical results for local refinement; non-matching grids.

The computational results are summarized in Table 5. One notices that for our interior penalty approximation the numerical experiments show that the local refinement reduces the L^2-error according to the theory, the error in the maximum norm is slightly better than one may expect and the error in H^1-norm is slightly worse than expected.

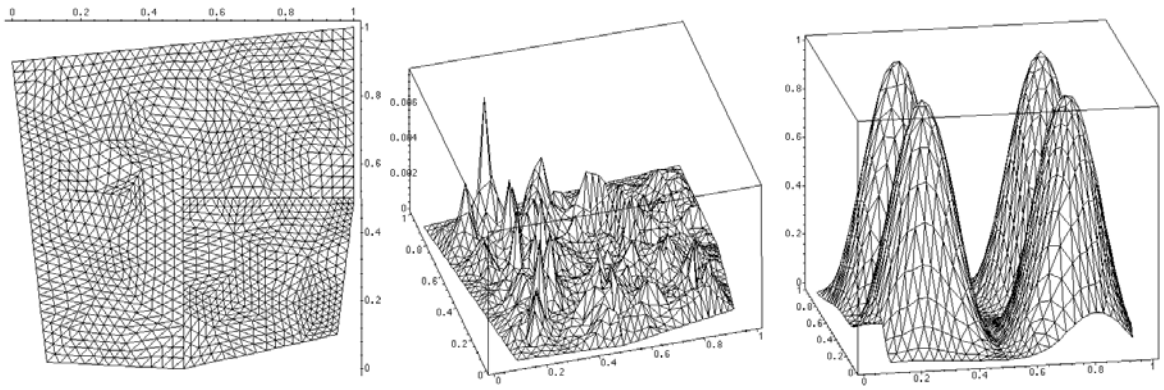

FIGURE 3. Mesh on level 3 (left), the error (middle) and the approximate solution on the same level (right).

5.4. **Results for variable discontinuous coefficient matrix a.** In this subsection we take $a_1 = I$,

$$a_2 = \begin{pmatrix} 1 + 10x^2 + y^2 & 0.5 + x^2 + y^2 \\ 0.5 + x^2 + y^2 & 1 + x^2 + 10y^2 \end{pmatrix},$$

and assume homogeneous Dirichlet boundary conditions on the whole boundary. The exact solution is $u(x, y) = sin^2(2\pi x)sin^2(2\pi y)$. The exact solution and the interior boundary are chosen such that the flux across the interior boundary is zero, hence $a\nabla u \cdot \mathbf{n} = 0$ on Γ. The domain is shown on Figure 3 (left). On the finest (5th)

Level	# nodes	L^∞-error	L^2-error	H^1-error	condition #
1	67	0.054202	0.052853	1.438307	113
	34	0.033052	0.022632	0.732204	
2	234	0.021709	0.014553	0.756781	511
	113	0.010203	0.006460	0.391482	
3	871	0.007720	0.003771	0.384874	2405
	409	0.003406	0.001670	0.198680	
4	3357	0.002486	0.000953	0.193395	10937
	1553	0.001223	0.000422	0.099706	
5	13177	0.000756	0.000239	0.096832	45853
	6049	0.000409	0.000106	0.049897	
order	2	1.5	2	1	2

TABLE 6. Numerical results for discontinuous coefficient matrix a; non-matching grids.

refinement level the error is 0.08%, 0.07% and 2.93% respectively in maximum, L^2 and H^1-norms. For this particular solution the error is second order in L^2-norm and

first order in H^1-norm. This should be expected since the main contributor to the error of our method is the term $a\nabla u \cdot \mathbf{n}$ along Γ, which in the case is zero.

5.5. **Estimates for the condition numbers.** The given in this section results are for the problem solved in subsection one. The meshes are non-matching and uniform refinement is used. Table 7 compares the condition numbers for matrices corresponding to the original problem (2.4), the reduced problem (4.1), the further reduced problem (4.3), and the further reduced problem (4.3) preconditioned with S_1^{-1} (see Section 4). As one can see in Table 7, the condition numbers behave like:

Condition Numbers					
Level	# nodes	1	2	3	4
1	65 31	149	13	4	1.90
2	225 102	519	26	8	1.93
3	833 367	2278	54	16	2.15
4	3201 1389	9781	108	35	2.46
5	12545 5401	40083	215	70	2.57
order	2	2	1	1	0

TABLE 7. In columns 1, 2, 3 and 4 we give the condition numbers for the problems (2.4), (4.1), (4.3), and (4.3) preconditioned with S_1^{-1}, respectively

$\mathcal{O}(h^{-2})$ for the original problem, $\mathcal{O}(h^{-1})$ for both (non–preconditioned) reduced problems, and $\mathcal{O}(1)$ when the preconditioner from Section 4 is applied, all in good agreement with the theory.

Acknowledgment. Part of this research has been done during the summer visits of the first and the second authors to Lawrence Livermore National Laboratory. The authors thank the Institute for Scientific Computing Research and the Center for Applied Scientific Computing for their hospitality and for the technical and financial support.

REFERENCES

[1] T. Arbogast, L. C. Cowsar, M. F. Wheeler, and I. Yotov, Mixed finite element methods on non-matching multi-block grids, SIAM J. Numer. Anal., **37** (2000) 1295–1315.

[2] D. Arnold, An interior penalty finite element method with discontinuous elements, SIAM J. Numer. Anal. **19** (1982) 742–760.

[3] I. Babuška, The finite element method for elliptic equations with discontinuous solutions, Computing, **5** (1970), 207–213.

[4] I. Babuška and W. C. Rheinboldt, Error estimates for adaptive finite element computations. SIAM J. Numer. Anal., **15** (1978) 736–754
[5] R. E. Bank and R. K. Smith, A posteriori error estimates based on hierarchical bases. SIAM J. Numer. Anal., **30** (1993) 921–932
[6] R. Becker, C. Johnson, and R. Rannacher, Adaptive error control for multigrid finite element methods. Computing, **55** (1995) 271–288
[7] J. H. Bramble, J. E. Pasciak, and P. S. Vassilevski, Computational scales of Sobolev norms with application to preconditioning, Math. Comp., **69** (2000) 463–480
[8] Y. Cao and M. D. Gunzburger, Least–squares finite element approximations to solutions of interface problems, SIAM J. Numer. Anal., **35** (1998) 393–405
[9] J. Douglas and T. Dupont, Interior penalty procedures for elliptic and parabolic Galerkin methods, Lecture Notes in Physics, **58** (1978) 207–216
[10] K. Eriksson and C. Johnson, An Adaptive Finite Element Method for Linear Elliptic Problems. Math. Comp., **50** (1988) 361–382
[11] R. D. Lazarov, J. E. Pasciak, and P. S. Vassilevski, Iterative solution of a coupled mixed and standard Galerkin discretization method for elliptic problems, Numer. Lin. Alg. Appl., (to appear).
[12] R. D. Lazarov, J. E. Pasciak, and P. S. Vassilevski, Mixed finite element methods for elliptic problems on non–matching grids, in *Large-Scale Scientific Computations of Engineering and Environmental Problems II* (M. Griebel et al., Eds.), Vieweg, Notes on Numerical Fluid Mechanics, **73** (2000), 25-35
[13] J. L. Lions and J. Peetre, Sur une class d'espaces d'interpolation, Institute des Hautes Etudes Scientifique, Publ. Math., **19** (1994) 5–68
[14] B. Rivière, M. Wheeler, and V. Girault, Part I. Improved energy estimates for the interior penalty, constrained and discontinuous Galerkin methods for elliptic problems, Computational Geosciences, **4** (2000) (to appear).
[15] T. Rusten, P. S. Vassilevski, and R. Winther, Interior penalty preconditioners for mixed finite element approximations of elliptic problems, Math. Comp., **65** (1996), 447–466.
[16] R. Verfürth, A posteriori error estimators for convection-diffusion equations, Numer. Math., **80** (1998) 641–663
[17] C. Wieners and B. I. Wohlmuth, The coupling of mixed and conforming finite element discretizations, in *Domain Decomposition Methods 10* (J. Mandel, C. Farhat, and X.-C. Cai, Eds.), Contemporary Math., # 218 (1998), AMS, pp. 547–554.
[18] O. C. Zienkiewicz and J. Z. Zhu, A Simple Error Estimator and Adaptive Procedure for Practical Engineering Analysis. Int. J. Numer. Meth. Engng., **24** (1987) 337-357

Department of Mathematics, Texas A & M University, College Station, TX 77843, U.S.A.
E-mail address: lazarov@math.tamu.edu

Department of Mathematics, Texas A & M University, College Station, TX 77843, U.S.A.
E-mail address: tomov@math.tamu.edu

Center for Applied Scientific Computing, Lawrence Livermore National Laboratory, Mail Stop L-560, 7000 East Avenue, Livermore, CA 94550, U.S.A.
E-mail address: panayot@llnl.gov